JOURNAL OF VIROLOGY, July 2002, p. 7049–7059 Vol. 76, No. 14
0022-538X/02/$04.00+0 DOI: 10.1128/JVI.76.14.7049–7059.2002

Complementary Roles of Multiple Nuclear Targeting Signals in the Capsid Proteins of the Parvovirus Minute Virus of Mice during Assembly and Onset of Infection

Eleuterio Lombardo,† Juan C. Ramírez, Javier Garcia,‡ and José M. Almendral*

Centro de Biología Molecular "Severo Ochoa" (Consejo Superior de Investigaciones Científicas-Universidad Autónoma de Madrid), 28049 Cantoblanco, Madrid, Spain

Received 28 January 2002/Accepted 6 April 2002

This report describes the distribution of conventional nuclear localization sequences (NLS) and of a beta-stranded so-called nuclear localization motif (NLM) in the two proteins (VP1, 82 kDa; VP2, 63 kDa) forming the T=1 icosahedral capsid of the parvovirus minute virus of mice (MVM) and their functions in viral biogenesis and the onset of infection. The approximately 10 VP1 molecules assembled in the MVM particle harbor in its 142-amino-acid (aa) N-terminal-specific region four clusters of basic amino acids, here called BC1 (aa 6 to 10), BC2 (aa 87 to 90), BC3 (aa 109 to 115), and BC4 (aa 126 to 130), that fit consensus NLS and an NLM placed toward the opposite end of the polypeptide (aa 670 to 680) found to be necessary for VP2 nuclear uptake. Deletions and site-directed mutations constructed in an infectious MVM plasmid showed that BC1, BC2, and NLM are cooperative nuclear transport sequences in singly expressed VP1 subunits and that they conferred nuclear targeting competence on the VP1/VP2 oligomers arising in normal infection, while BC3 and BC4 did not display nuclear transport activity. Notably, VP1 proteins mutated at BC1 and -2, and particularly with BC1 to -4 sequences deleted, induced nuclear and cytoplasmic foci of colocalizing conjugated ubiquitin that could be rescued from the ubiquitin-proteasome degradation pathway by the coexpression of VP2 and NS2 isoforms. These results suggest a role for VP2 in viral morphogenesis by assisting cytoplasmic folding of VP1/VP2 subviral complexes, which is further supported by the capacity of NLM-bearing transport-competent VP2 subunits to recruit VP1 into the nuclear capsid assembly pathway regardless of the BC composition. Instead, all four BC sequences, which are located in the interior of the capsid, were absolutely required by the incoming infectious MVM particle for the onset of infection, suggesting either an important conformational change or a disassembly of the coat for nuclear entry of a VP1-associated viral genome. Therefore, the evolutionarily conserved BC sequences and NLM domains provide complementary nuclear transport functions to distinct supramolecular complexes of capsid proteins during the autonomous parvovirus life cycle.

The nuclear membrane offers a second barrier to those viruses that, upon specific cell surface recognition and internalization, need components of the replication and transcription machinery of the host cells for their multiplication. Indeed the structural components of karyophilic viruses reach the nucleus at two stages of the life cycle, first when the incoming particle delivers the genome and late in the infection during the nuclear accumulation of viral components leading to the biogenesis of the virions. As for the cellular components, the nuclear import of viral macromolecules must proceed across the central aqueous channel of the nuclear pore complex (NPC) (18, 58), a large structure with an eightfold rotational symmetry built from proteins called nucleoporins. Cytoplasmic-nuclear transport is directed by the interaction of a subset of nucleoporins with soluble shuttling factors (reviewed in reference 46) recognizing nuclear localization sequences (NLS; reviewed in reference 24) present in most karyophilic polypeptides. The conventional NLS is formed by a short stretch of basic amino acids in either a single domain (33, 34) or two domains (54) which are recognized by transport receptors of the importin/karyopherin family (46). But nonconventional NLS do not fit a consensus (43, 51, 55), may adopt a structured configuration (38), and bind different families of import receptors (40). Understanding the mechanisms of viral nuclear transport may allow the identification of intracellularly acting host range and tropism determinants.

Conventional and nonconventional NLS are being described in viral structural proteins synthesized de novo (e.g., references 31 and 67), though their roles in the nuclear entry of karyophilic viral particles during natural infection and the mechanisms regulating the process are still poorly understood. The 25-nm functional diameter of the NPC central channel (22) may allow the elongated baculovirus nucleocapsid to pass through (63), but the larger capsid of most nuclear viruses must undergo a partial or total disassembly process to deliver the genome into the nucleus (reviewed in references 35 and 68). Thus, RNA viruses, such as influenza virus, completely disassemble, releasing ribonucleoproteins into the cytoplasm (11), and retroviruses capable of targeting the nuclei of nondividing cells generate a subviral preintegration complex that translocates mainly by virtue of a nonconventional NLS of the integrase enzyme (9) and an unusual short DNA overlap

* Corresponding author. Mailing address: Centro de Biología Molecular "Severo Ochoa" (CSIC-UAM), Universidad Autónoma de Madrid, 28049 Cantoblanco, Madrid, Spain. Phone: 34-91-3978048. Fax: 34-91-3978087. E-mail: jmalmendral@cbm.uam.es.

† Present address: The Scripps Research Institute, La Jolla, CA 92037.

‡ Present address: Instituto de Salud Carlos III, 28220 Madrid, Spain.

TABLE 1. Point mutations introduced in the MVMi capsid proteins

Mutated domain	Amino acid change(s)[a]	Mutagenic oligonucleotides[b] (5′ → 3′)
ΔBC 1	R7**T**; K9**N**	CCTCT**G**TTAGCT**G**TTTTAGC
	K6**N**; R10**N**	CCT**G**TGTTAGCTGT**G**TTAGCTGG
ΔBC2	K89**N**; R90**S**	GCAAAAGCGC**TG**TTGGTTC
ΔNLM	K672**N**; R676**T**	TGCT**G**TCATTGTTAG**A**TTCC
	G671**P**	CTCATTGTTAGTTTT**GG**TTTCCAGAAAAATGTACC

[a] Numbers start from the amino terminus of VP1. Amino acid changes are in boldface.
[b] Oligonucleotides are complementary to the coding strand, and the introduced nucleotide changes are indicated in boldface.

formed during reverse transcription (72). The spherical nucleocapsid of the large DNA viruses docks at the nuclear pore and releases the genome either by a conformational change without disassembly, as in herpesvirus (47), or by a complete disassembly upon docking at the CAN/Nup214 fibril nucleoporin and further binding to histone H1 and H1 import factors, as in adenovirus type 2 (60). Even for the smaller capsid of papovavirus, an identified NLS in the minor capsid protein (31), presumably internal to the virus structure (37), suggested a major conformational change of the capsid so that the signal becomes accessible to the transport machinery (45).

The nonenveloped capsid of the *Parvoviridae*, a family of single-stranded DNA (5-kb) nuclear viruses with diameters close to 25 nm (6, 16), could physically traverse the NPC in an intact configuration. It is controversial whether structural protein subunits synthesized de novo are transported for nuclear capsid assembly to occur (30, 38, 69) or whether cytoplasmic assembly precedes nuclear invasion (70), as transport domains could be formed at the capsid surface. Indirect support for this hypothesis may be derived from the tropism determinants mapped at the capsid surface of the incoming parvoviral particle (3, 25, 26, 50, 52) and from the possibility of blocking the transit of canine parvovirus (CPV) virions across the cytosol in natural infection by the microinjection of neutralizing antibodies (65). However, the two capsid proteins of the parvovirus minute virus of mice (MVM), the larger VP1 (83 kDa) and the major VP2 (63 kDa), were able to translocate to the nucleus when singly expressed in transfected cells, though only VP2 assembled in capsids (62), indicating that both polypeptides have an NLS whose activity is, at least for VP1, independent of capsid formation. The general interest of the parvoviral system for nuclear transport studies lies in the fact that, unlike most karyophilic viruses (except some papovaviruses [37]), a high-resolution three-dimensional structure of the T=1 icosahaedral capsid is available for MVM (1), CPV (61), and other parvoviruses, and thus an identified NLS may be placed in the capsid context and putative conformational changes of the coat to access the nuclear transport machinery can be predicted. In the crystal structure of the MVM capsid (1), an ordered symmetry has been resolved for approximately 35% of the DNA genome and most of the VP1/VP2 common polypeptide chain, but the order is lost at residue 40 of VP2, so the configurations of the N termini of both polypeptides are unknown. Protease digestions and accessibility to antibodies in pure preparations of parvovirus particles indicated that the VP1 N-terminal peptide is internal to the capsid (15) and that the VP2 N terminus is exposed in DNA-filled particles but not in empty ones (48, 59).

We have addressed the issues of the assembly pathway and nuclear targeting of the autonomous parvoviruses, pursuing the functional identification of the nuclear import sequences in the capsid proteins of strain i of MVM (MVMi) (8), a pathogenic virus of newborn and immunodeficient mice (10, 53, 57). MVMi capsid is formed from approximately 10 subunits of VP1 and 50 subunits of VP2, the entire VP2 coding sequence being contained in VP1, which has an additional specific 142-amino-acid sequence at its N terminus (59). The VP1/VP2 ratio in the capsid is fixed at the protein level in the infected cell, which is itself regulated mostly by the splicing rate of the R3 messengers resulting from the P38 promoter (13, 32, 44, 56). VP2 targets the nucleus by a structured so-called nuclear localization motif (NLM) formed at one of the eight β-strands of the β-barrel topology of the capsid, which drives into the nucleus singly expressed VP2 subunits, as well as VP1/VP2 oligomers (38). The VP1-specific sequence contains four stretches of basic amino acids highly homologous to conventional NLS that were hypothesized to act as nuclear targeting sequences for the protein and for the MVM virions (62). Indeed, it has recently been shown for CPV that microinjected antibodies against the VP1 unique region can neutralize infection, and mutations within the VP1 N-terminal sequence reduce virus multiplication in culture (66).

This report describes a genetic analysis in MVM of (i) the nuclear transport capacity of the NLM and of the four basic domains of the VP1-specific N terminus for VP1 subunits synthesized de novo and for the VP cytoplasmic complexes formed in the infected cell, (ii) the relationship of the transport process with subcellular capsid assembly, and (iii) the role played by these sequences in the delivery of the incoming viral genome to the nucleus. Collectively, the functions of the different capsid transport sequences are shown to be complementary for the nuclear assembly of an infectious MVM particle and for the initiation of an infection cycle by processes involving protein ubiquitination and viral coat structural transitions, respectively.

MATERIALS AND METHODS

MVMi deletion and site-directed mutants. The entire set of mutations was constructed in an infectious plasmid of the MVMi genome (pMVMi [25]). Plasmids were transformed and amplified in *Escherichia coli* strain JC8111, which permits deletion-resistant propagation of MVM plasmid clones bearing terminal palindromes (7). Deletion mutants across the VP1-specific N-terminal region were constructed by cutting pMVMi at the single *Hin*dIII site of the MVMi genome (4) followed by serial digestion with *Bal*31 nuclease (1 U/μg of DNA; Roche) and ligated, and an in frame deletion mutant was selected by DNA sequencing. Point mutations were engineered by oligonucleotide-directed mutagenesis following the procedure described by Kunkel (36) and using the *E. coli* CJ236 and JM109 strains for mutant selection. The point mutations introduced for the removal of amino acids at specific domains of the VP proteins are indicated in Table 1. To mutate the N-terminal VP1-specific region, an *Eco*RI

restriction fragment (nucleotides [nt] 1080 to 3500) of pMVMi was cloned in the M13mp18 phage vector, and the single strand was used as a template for the mutagenesis reactions. The mutations were then transferred to pMVMi or other derived mutant plasmids by exchanging the *Xho*I-*Spe*I fragment (nt 2075 to 3001) for the mutated fragment. The insertion of site-directed mutations that inactivate the NLM common to VP1 and VP2 (ΔNLM mutants) and the construction of an MVMi mutant not expressing the VP1 protein (ΔVP1/VP2) have been previously described (38). An MVMi mutant not expressing the VP2 protein (VP1/ΔVP2) was obtained by introducing point mutations at the minor splicing donor site D1, as explained in Results (Fig. 1), and the same mutations were also used in the series of mutants expressing only VP1 (Fig. 2). The amino acid and nucleotide changes were numbered from the start of VP1, and their positions in the virus genome (4) are indicated in Table 1. Mutants were sequenced in the M13mp18 phage vector by the dideoxy-mediated chain termination method incorporating [^{35}S]dATP with T7 DNA polymerase (Pharmacia) and were verified in the double-stranded plasmid DNA preparations to be used for cell transfection with an automatic sequencer (Perkin-Elmer model 377). Sequencing and mutagenic oligonucleotides were purchased from Isogen Bioscience BV (Maarssen, The Netherlands).

Transfection. The human simian virus 40-transformed fibroblast cell line NB324K, permissive for MVMi productive infection (25) and selected for maximum susceptibility (38), was transfected by electroporation with plasmid preparations enriched in supercoiled forms by chromatography (Qiagen). The cells were trypsinized and resuspended at a density of 2×10^7 per ml in Dulbecco modified Eagle medium (DMEM) (Gibco-BRL) and 5% heat-inactivated fetal calf serum (FCS) (Gibco-BRL). After cooling for 15 min at 4°C, 0.15 ml of cells was added to 10 μg of plasmid and 25 μg of carrier salmon sperm DNA, and the mixture was electroporated in a 0.4-cm-diameter cuvette by applying one pulse at 230 V and 250 μF using a Gene Pulser apparatus with capacitance extender (Bio-Rad). The cells were immediately diluted in DMEM with 5% FCS and seeded at several densities on 60-mm-diameter dishes. The adhered cells were extensively washed with phosphate-buffered saline (PBS) 14 h posttransfection, and the medium was replaced with fresh DMEM–5% FCS growth medium supplemented with a 10-fold excess of a neutralizing dilution of MVM capsid antiserum (α-MVM) to block reinfection of putatively produced infectious particles.

Antibodies. A rabbit polyclonal antiserum (α-VP1) raised against the 141 amino acids of the entire VP1-specific N-terminal region expressed in *E. coli* as a protein fragment (15) was used for the immune recognition of VP1. For the general localization of both VP1 and VP2 capsid proteins, the VP antigen, an antiserum (α-VPs) raised against denatured VP2, was used (to be described elsewhere). The preparation and use of a rabbit antiserum raised against gradient-purified MVM empty particles (α-MVM) and of a mouse anti-MVM intact capsid monoclonal antibody (MAb) (α-Capsid) have been recently described (38). A mouse MAb (MAb FK2 [23]) recognizing polyubiquitinylated and monoubiquitinylated proteins but not free ubiquitin (Ub), was purchased from Affinity Research Products (Manhead, United Kingdom).

Immunological analyses. For subcellular localization of the several antigens by double-label indirect immunofluorescence (IF) in conventional and confocal microscopy, NB324K cells seeded onto glass coverslips were washed twice with PBS 40 to 48 h posttransfection and fixed in methanol-acetone (1:1) at −20°C for 7 min. After blocking the cells in 20% horse serum, primary antiserum (α-VP1, α-MVM, or α-VPs) or the anti-MVM capsid MAb (α-Capsid) was applied diluted 1:200 or 1:20, respectively, in PBS supplemented with 5% horse serum for 45 min at 37°C. The bound immunoglobulin G was visualized with a goat anti-rabbit antibody conjugated to Texas red or with a goat anti-mouse antibody conjugated to fluorescein isothiocyanate (Jackson Immuno Research Laboratories, Inc.) (used at 1/200). Samples were dehydrated with ethanol and mounted in Mowiol 4-88 (Hoechst). Phenotypes were scored with a Zeiss Axiophot microscope from monolayers grown to subconfluence and showing a significant proportion of transfected cells. Confocal microscopy was performed using a Radiance 2000 laser scanning microscope with two lasers giving excitation lines at 488 (fluorescein isothiocyanate) and 543 nm (Texas red). Data from the channels were collected sequentially at a resolution of 1,024 by 1,024 pixels using optical slices between 0.5 and 1 μm thick.

To determine VP expression in transfected cells by immunoprecipitation, the cultures were labeled from 14 to 40 h posttransfection with 250 μCi of [^{35}S]methionine-[^{35}S]cysteine (Pro-mix; Amersham)/ml in methionine-free DMEM–10% dialyzed FCS supplemented with 10% normal medium. The cells were washed twice with cold PBS, scraped into 150 mM NaCl–50 mM Tris (pH 8.0)–1% NP-40–0.3% sodium dodecyl sulfate (SDS)–0.5% β-mercaptoethanol, and incubated overnight at 4°C with a 1/100 dilution of the specific antiserum. Immune complexes were precipitated with protein A-Sepharose (10% [wt/vol]) and washed with cold PBS, 0.05% NP-40, and 1% BSA, and bound proteins were subjected to 10% SDS-polyacrylamide gel electrophoresis. The gels were fixed, dried, and exposed for autoradiography to Kodak X-Omat films.

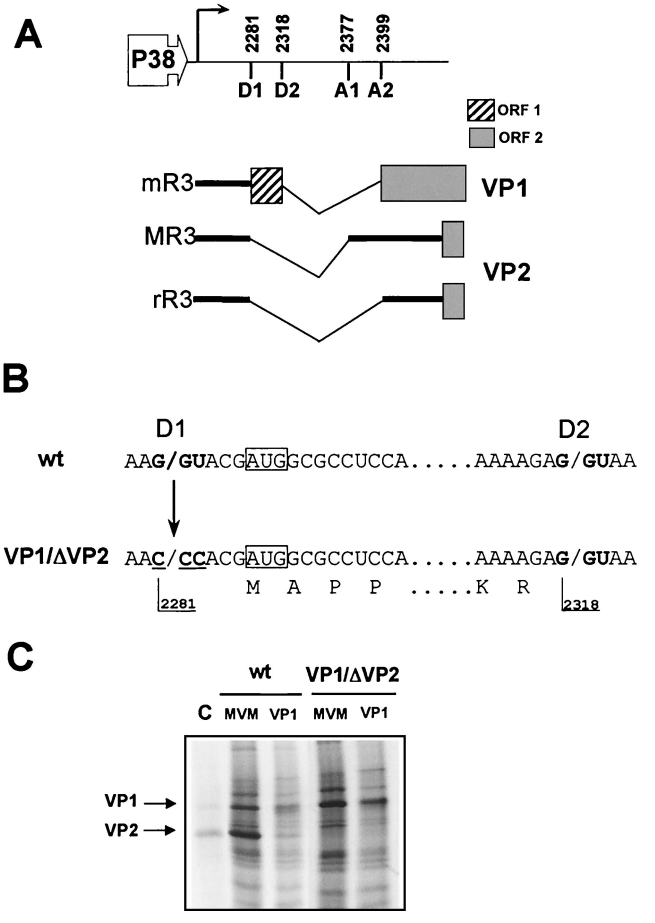

FIG. 1. Construction of a VP-1-only MVM genome. (A) Genome organization of the parvovirus MVM in the minor intron region. The P38 promoter and the positions of the two donor (D1 and D2) and the two acceptor (A1 and A2) sites of splicing are indicated using MVMi numbering. VP1 is made from a minor mR3 species that results from the use of the D2 donor (nt 2318) and the A2 acceptor (nt 2399), whereas most viral transcripts are spliced at the D1 donor (nt 2281), thus omitting the VP1 start codon, yielding messengers MR3 and rR3 that use either A1 (nt 2377) or A2 acceptors and express the major VP2 protein. ORF, open reading frame. (B) Inactivation of the minor splicing donor D1 of the MVM genome. The VP1 start codon and the three point genetic changes introduced in the donor splicing site 1 (D1) to produce the mutant plasmid VP1/ΔVP2 are underlined. For simplicity, the alterations that these mutations introduce in the carboxy-terminal region of the NS2 protein isoforms (17) generated from the R2 messengers have not been outlined. (C) Pattern of VP protein expression from the MVM splice donor mutant genome. Protein extracts from NB324K cells transfected with the indicated plasmids and metabolically [^{35}S]Met labeled 16 to 48 h posttransfection were immunoprecipitated with capsid antiserum (MVM) or with serum raised against the VP1-specific N-terminal sequence (VP1). The positions of the VP proteins obtained from [^{35}S]Met-labeled and gradient-purified MVMi capsid (C) are indicated on the left.

Measurement of MVMi particle infectivity. To grow the VP1 virus mutants, 9×10^6 NB324K cells were electroporated with 30 μg of each plasmid construct DNA as described above, seeded at a density of 1.5×10^6 per 90-mm-diameter dish, and washed, and fresh medium was substituted 8 h afterwards. The cell monolayers were scraped 72 h posttransfection into 50 mM Tris (pH 7.5)–2 mM EDTA containing 0.25% SDS, and the homogenates were subjected to a stan-

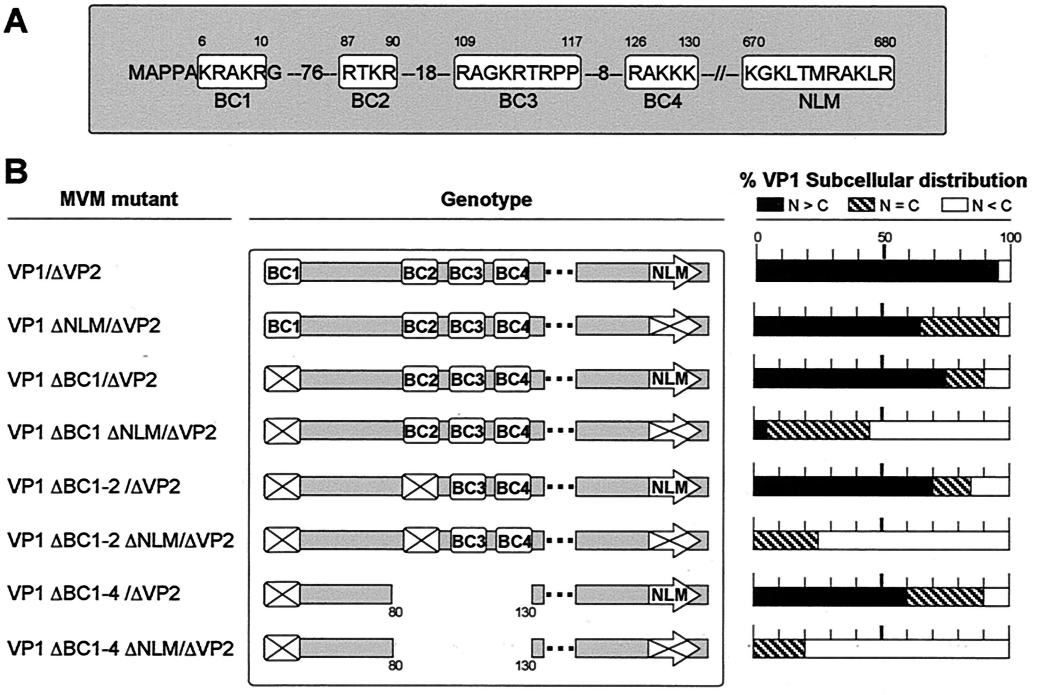

FIG. 2. VP1 nuclear targeting sequences. (A) Distribution of basic amino acid sequences along the VP1 protein. The four clusters of basic sequences (BC1 to BC4) in the VP1-specific N-terminal domain and the NLM in the carboxy-terminal region shared with VP2 are indicated. (B) Subcellular localization of the VP1 mutant proteins. Shown are the nomenclature and genotypes of the genomic MVMi mutants constructed in the VP1 basic sequences and the subcellular distribution of the VP1 mutant proteins in the transfected-cell population. Inactivating mutations in the BC sequences (boxes) and in the NLM (arrows) are represented by crosses. The percentages are the average values from more than 300 stained cells scored 40 to 48 h posttransfection from at least two independent experiments. The phenotypes were examined by epifluorescence with a Zeiss Axiophot microscope and classified in three categories: mostly nuclear (N > C), mixed (N = C), and cytoplasmic (N < C).

dard procedure to purify MVM particles by centrifugation through a sucrose cushion and CsCl equilibrium centrifugation as described previously (39). Fractions were collected from the tops of the gradients, and those corresponding to the density of MVM DNA-filled particles (1.39 to 1.41 g/ml) were pooled and extensively dialyzed against PBS. Mutant and wild-type (wt) purified MVMi virion particles were quantitatively tested for infectivity by inoculating NB324K cell monolayers with preparations performed in parallel and adding an excess of neutralizing antibody (α-MVM) 6 h postinfection (p.i.) to block putative reinfection. The number of particles in the purified inocula was normalized for the single-stranded signal of the virion genomes obtained in control Southern blots. Viral genome replication was monitored from 10^6 growing NB324K cells inoculated with purified virions for 1 h at 37°C in PBS, extensively washed, and then processed for low-molecular-weight DNA extraction (42) either immediately (0 h p.i.) or at a late infection time (24 h p.i.). The synthesis of viral replicative intermediates was quantitatively determined by Southern blotting with an MVM ^{32}P-labeled DNA probe as previously described (53). The number of cells showing VP protein expression (fluorescent focus) was determined 24 h postinoculation of cellular monolayers grown on coverslips by IF staining with α-VPs antiserum as described above.

RESULTS

VP1 contains multiple, dispersed nuclear transport sequences. To quantitatively analyze VP1 nuclear targeting capacity in the context of viral genome regulation, but precluding VP2 cooperative interaction for nuclear import (38), point mutations were introduced to inactivate the D1 consensus sequence (32, 44) in an MVMi infectious plasmid. This strategy suppresses the synthesis of the characteristic carboxy ends of the NS2 isoforms P and L and introduces two point mutations in the Y isoform (17), but it preserves most NS2 protein sequence, which contributes to MVM capsid assembly in murine cells (14). Mutations were selected according to the method of Green (27) in the almost invariant eukaryotic G/GU trinucleotide at the 5′ splice site to completely inactivate its function as a splicing donor (Fig. 1B), and the resulting plasmid (VP-1/ΔVP2) was tested for VPs expression. As shown in Fig. 1C, transfection with wt infectious plasmid yielded VP1 and VP2 proteins at a physiological ratio, but cells transfected with the VP-1/ΔVP2 plasmid lacked VP2 expression, though VP1 subunits of the correct size accumulated normally.

The distribution of sequences with nuclear targeting capacity across the VP1 protein was investigated with a series of mutations created in the four basic clusters (BC) of the VP1 N-terminal-specific region (here called BC1 to BC4) and in the NLM domain (Fig. 2A). Singly expressed VP1 subunits (VP1/ΔVP2 mutant) efficiently localized in the nuclei of all transfected cells (Fig. 2B). Significantly, the inactivation of the NLM (mutations K672N, R676T, or G671P; Table 1) produced mostly VP1 nuclear proteins (VP1ΔNLM/ΔVP2 mutant), though some cytoplasmic retention was noted in approximately one-third of the transfected cells. Thus, unlike for VP2 (38), the NLM is not the only sequence with VP1 nuclear transport capacity. Mutations were next introduced in the four BC sequences of VP1 (Fig. 2B), as BC1 and BC2 are highly homologous to single conventional NLS (33, 34), and BC3-BC4 with an 8-amino-acid spacing sequence in between may form a bipartite NLS (54). The mutation of BC1 alone (mutations

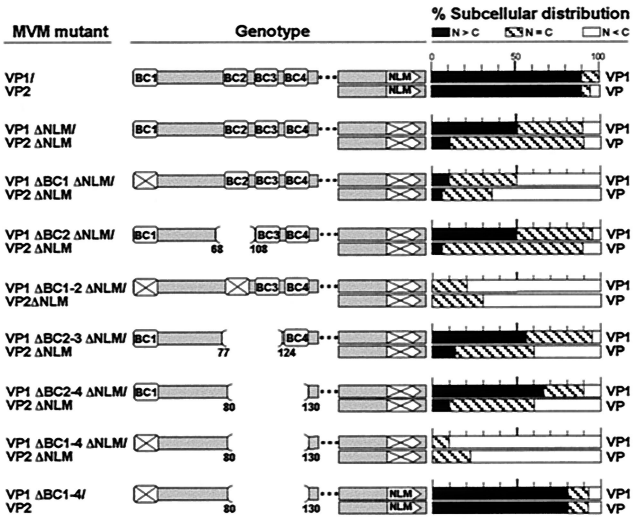

FIG. 3. Sequences involved in the nuclear targeting of VP1/VP2 complexes. Shown are a series of MVMi site-directed and deletion mutants constructed in the VP1-specific BC sequences and in the NLM domain. For the sake of simplicity, other viral genotypes carrying VP1 mutations close to the ΔBC2-3 (89-125 deletion mutant) or the ΔBC1-4 (80-128 deletion mutant) giving similar phenotypes are not depicted. Genomic plasmids carrying the indicated mutations were transfected into NB324K cells, and the subcellular distributions of VP1 and of the VP antigen (VP1 plus VP2) were monitored in the same cells 40 to 48 h afterwards by IF with the α-VP1 and α-VPs antisera, respectively. Phenotypic characterization was performed as for Fig. 2.

K6N, R7T, K9N, and R10N; Table 1) had some minor effect on VP1 nuclear transport, but when combined with NLM inactivation (VP1ΔBC1ΔNLM/ΔVP2 mutant), it determined a predominant or exclusive VP1 cytoplasmic phenotype in most cells (Fig. 2B). A certain role for BC2 in VP1 subcellular localization became evident when the poorly nuclear phenotype of the VP1ΔBC1ΔNLM/ΔVP2 mutant was compared to the absence of cells with predominant nuclear staining in the VP1ΔBC1-2ΔNLM/ΔVP2 mutant. The latter mutant also showed the lack of nuclear transport activity in BC3 and BC4, a conclusion further supported by the null effect on VP1 transport of a large deletion that removed these sequences (see VP1ΔBC1-2ΔNLM/ΔVP2 versus VP1ΔBC1-4ΔNLM/ΔVP2 phenotype; Fig. 2). This study showed that VP1 harbors two independent major nuclear localization domains, BC1 and NLM, at its opposite ends which are necessary for the nuclear transport of most VP1 subunits synthesized de novo in the infected cell. In addition, BC2 behaved as a weak NLS, while BC3 and BC4 lack any significant nuclear transport activity.

Sequences driving the nuclear translocation of MVMi capsid protein oligomers. In a natural infection, VP1 is expressed at a 1/5 ratio with VP2 (16, 56), and the proteins cooperate for nuclear transport through cytoplasmic interaction (38). To investigate the activity of the VP1 NLS in the context of VP1/VP2 coexpression at the physiological ratio, a series of mutants were constructed in an infectious MVMi plasmid in which the individual VP1-specific BC sequences, and the NLM domain common to both VP1 and VP2 proteins, had been alternately inactivated by deletions or point mutations. A representative set of all the mutants used in this analysis is shown in Fig. 3. VP1, as well as most VP antigen (VP1 plus VP2), efficiently localized in the nuclei of cells transfected with the wt genome (VP1/VP2 [Fig. 3, top]). In the absence of the NLM (mutant VP1ΔNLM/VP2ΔNLM), which is absolutely required for the transport competence of the VP2 subunits (38), close to 90% of the transfected cells showed a nuclear or mixed phenotype for VP1. This percentage was matched by the subcellular distribution of the VP antigen, although there the mixed phenotype was predominant. On average, this pattern of subcellular distribution for the VP antigen was obtained in each of the mutants in which BC1 was present (e.g., mutant VP1ΔBC2-4ΔNLM/VP2ΔNLM), indicating that a significant fraction of the VP2ΔNLM subunits were carried into the nucleus by the less-abundant transport-competent VP1 subunits. In contrast, a predominant or exclusive cytoplasmic localization of VP1 and of the VP antigen was obtained in those mutants in which only BC3 and BC4 (mutant VP1ΔBC1-2ΔNLM/VP2ΔNLM), or none of the BC sequences (mutant ΔBC1-4ΔNLM/VP2ΔNLM), was present. Thus, the small percentage of cells showing a nuclear phenotype in the transfections with the ΔBC1ΔNLM/VP2ΔNLM mutant indicated a minor but significant nuclear transport capacity of BC2. Therefore, BC1 and BC2 display nuclear transport activity for VP1/VP2 complexes formed under a physiological expression ratio, while BC3 and BC4 do not harbor such activity. Finally, when the VP1-specific BC sequences had been deleted but competent VP2 subunits were coexpressed (mutant VP1ΔBC1-4/VP2), VP1, as well as most VP subunits, efficiently reached the nucleus (Fig. 3, bottom). This mutant clearly demonstrated that the NLM can act as an important nuclear targeting domain for VP complexes.

NLS and capsid subunit interactions contribute to MVMi assembly. To study the relationship between nuclear transport and capsid assembly, the entire series of constructed VP mutants was analyzed with specific antibodies and confocal microscopy for the capacity to form viral capsids. Figure 4 illustrates representative fields of cells from this study with nuclear or cytoplasmic phenotypes. Singly expressed VP1 protein (mutant VP1/ΔVP2) was unable to form capsids even under high nuclear accumulation (Fig. 4, left), in sharp contrast with the efficient capsid formation capacity of VP2 (see below), suggesting that some VP1-specific sequences preclude capsid formation. In a tentative attempt to map these sequences, the whole collection of MVM genomes with VP1 mutations and deletions and lacking VP2 expression (Fig. 2) was similarly analyzed. None of the mutants tested, even those with large deletions (e.g., mutant ΔBC1-4/ΔVP2), showed any trace of capsid formation as judged by α-Capsid monoclonal staining (Fig. 4, left), regardless of the subcellular compartment where VP1 accumulated. A VP1 punctuated staining appearing in some deletion mutants was not due to capsid formation, and its nature is discussed below.

The roles of the VP2 subunits in this process were investigated next. Singly expressed VP2 subunits (ΔVP1/VP2 mutant) efficiently translocated to the nucleus and assembled in capsids (Fig. 4, upper right), in agreement with the previously reported capacity of VP2 in several parvoviruses to form empty capsids in host and heterologous systems (12, 28, 62, 70). An interaction between both types of subunits for capsid assembly is illustrated in the VP1ΔBC1-4/VP2 mutant, as these deleted VP1 subunits showed a characteristic mixed phenotype when

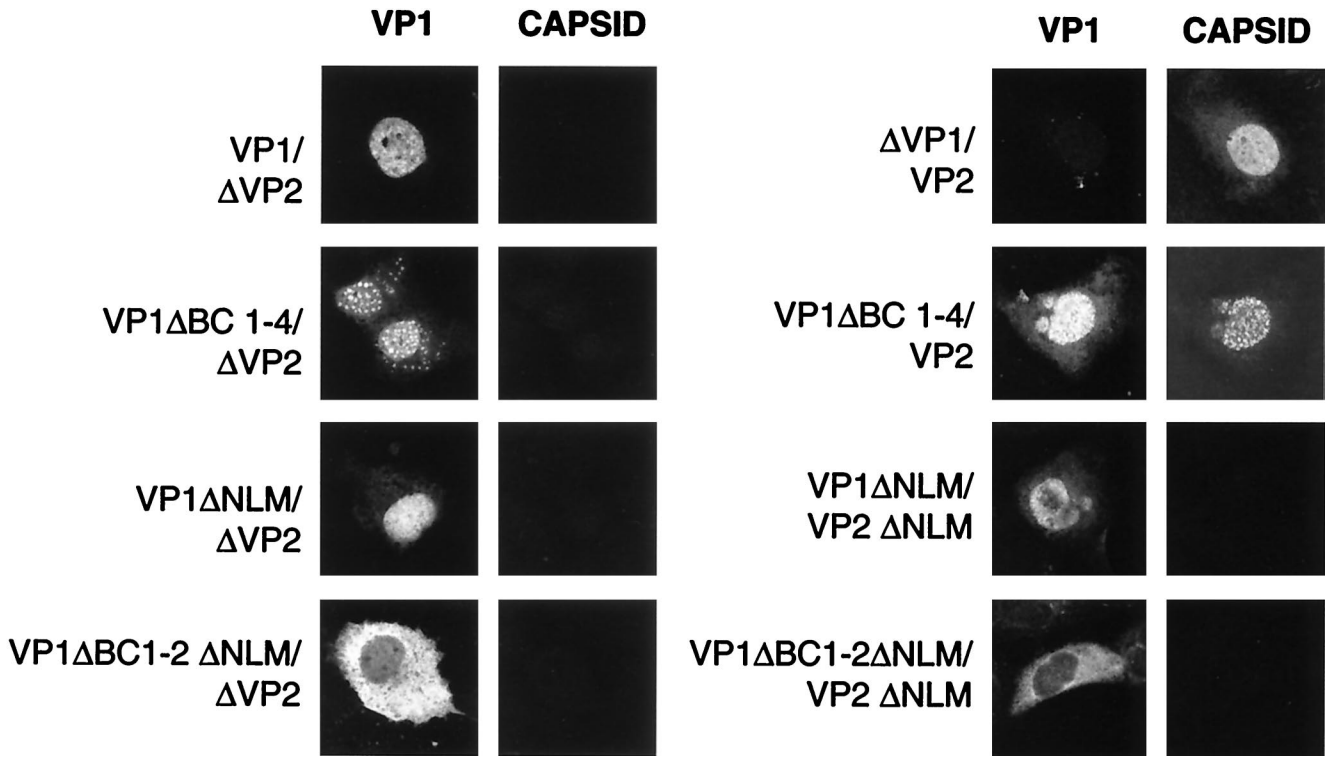

FIG. 4. Capsid formation by VP mutant proteins. Shown is an IF confocal analysis of the subcellular distribution of VP1 and MVMi capsid in cells transfected with the indicated viral plasmids. Double staining was done with a VP1-specific polyclonal antiserum (VP1) and with an MVM capsid MAb (CAPSID). The predominant phenotype for each of the indicated plasmids is shown. Left, VP1-only mutants; right, VP1 mutants with wt or mutant VP2 coexpression.

singly expressed (Fig. 4, left) but were quantitatively brought into the nucleus and colocalized with the capsid antigen in cells synthesizing VP2 subunits (Fig. 4, right). Similar results were obtained with the rest of the VP1 mutants carrying genetic changes in the BC sequences (not shown). However, capsid did not form when the interaction occurred between VP subunits lacking a functional NLM domain (ΔNLM mutants), under an absolute cytoplasmic retention (mutant VP1ΔBC1-2ΔNLM/VP2ΔNLM), or even when the activities of BC sequences determined significant nuclear transport of VP complexes (mutant VP1ΔNLM/VP2ΔNLM). Control experiments showed that coexpressed transport-incompetent VP2 subunits with distinct inactivating mutations in the NLM domain (Table 1) did not cooperate at all for nuclear transport (not shown). Therefore, MVMi capsid formation was always a nuclear event dependent upon the presence of transport-competent VP2 subunits.

VP1 N-terminal mutants induce the accumulation of colocalizing conjugated Ub. Several singly expressed VP1 mutants (ΔVP2) gave a characteristic mottled phenotype of protein accumulation with little or no diffuse staining. This phenotype appeared as cytoplasmic dots in the VP1ΔBC1-2ΔNLM protein (Fig. 5A) and as slightly larger nuclear dots in cells expressing the VP1ΔBC1-2 protein (not shown). Moreover, the sizes of VP1 accumulations increased with the extent of the deletion, forming striking big dots or irregular circles reactive with the MVM capsid antiserum in the cytoplasmic VP1ΔBC1-4ΔNLM protein (Fig. 5E), as well as in the nuclear translocated VP1ΔBC1-4 protein (Fig. 4, left). The percentage of cells in the transfected population showing the VP1 mottled phenotype increased with the size of the accumulations, ranging between approximately one-third in dots and two-thirds for the VP1 circles. NLM inactivation alone did not lead directly to dot formation (e.g., VP1ΔNLM/ΔVP2 mutant [Fig. 4, left]), though as indicated above, it influenced VP1 subcellular distribution and thus the sizes of the dots.

The morphology of the VP1 dots and circles resembled protein accumulations conjugated to Ub in the Ub-proteasome degradation pathway (21). To explore the possible ubiquitination of MVM capsid proteins, transfected cells were analyzed with MAb FK2, which specifically recognizes conjugated but not free monomer Ub (23) and which has been used to detect conjugated Ub by IF (2). Remarkably, the VP1 dots of the ΔBC1-2ΔNLM mutant protein (Fig. 5A and B) and the VP1 large dots and circles appearing in cells expressing the ΔBC1-4ΔNLM mutant protein (Fig. 5E and F) largely colocalized with conjugated-Ub staining. This pattern of conjugated-Ub accumulation colocalizing with the VP1 foci induced by the BC mutants was not apparent in the wt. Rather, the MAb FK2 staining of cells transfected with the infectious MVMi plasmid was diffused, as in the contiguous nontransfected cells (Fig. 5I and J), namely, a minor conjugated-Ub accumulation that varied among cells as previously reported (2, 21). Interestingly, the coexpression of cytoplasmic VP2 subunits (ΔNLM) removed the pattern of VP1 accumulation (Fig. 5C and G), as well as the foci of conjugated Ub (Fig. 5D and H). Indeed, the

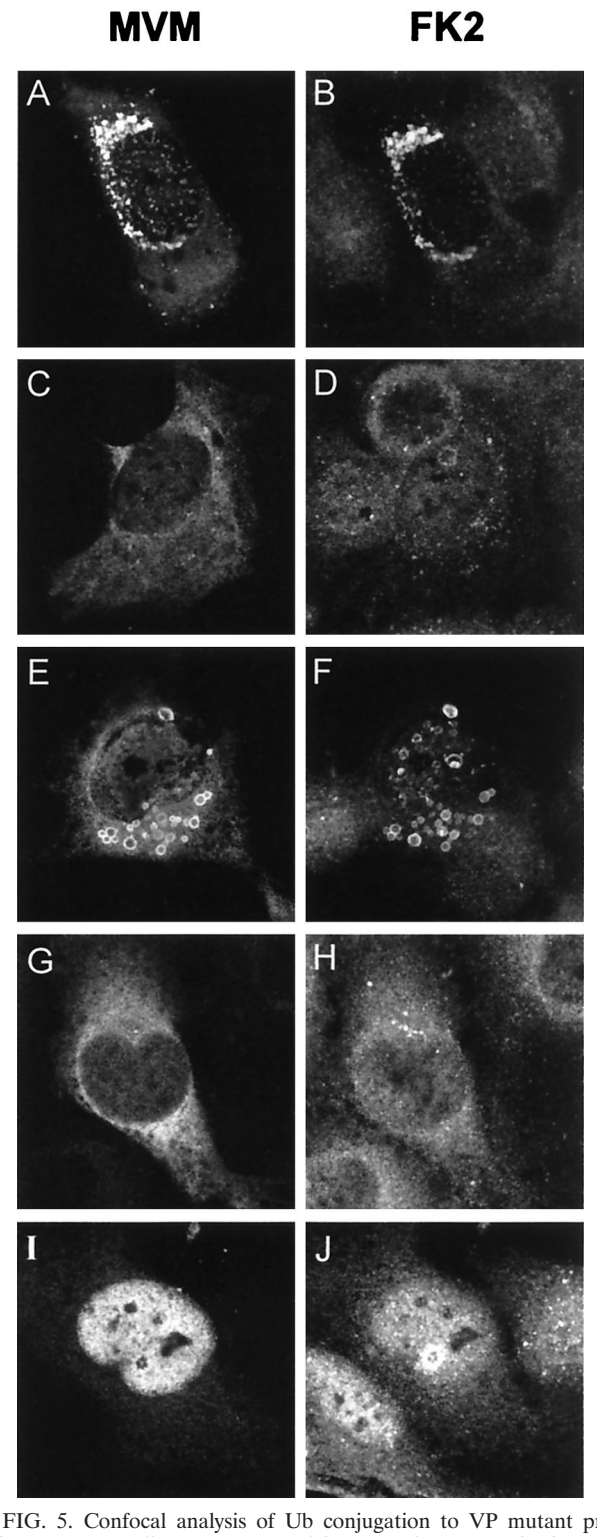

FIG. 5. Confocal analysis of Ub conjugation to VP mutant proteins. NB324K cells were processed for IF 40 h posttransfection and costained with an antiserum raised against MVM capsid (MVM; 1/200 dilution) and a MAb recognizing conjugated Ub (FK2; 1/500 dilution). The panels correspond to representative fields of cells transfected with the following plasmids: VP1ΔBC1-2ΔNLM/ΔVP2 (A and B), VP1ΔBC1-2ΔNLM/VP2ΔNLM (C and D), VP1ΔBC1-4ΔNLM /ΔVP2 (E and F), VP1ΔBC1-4ΔNLM/VP2ΔNLM (G and H), and wt MVMi (I and J).

FK2 staining resembled that of nontransfected cells. A similar VP2-mediated prevention of conjugated-Ub and VP1 accumulations was also apparent in the nucleus when the VP1 mottled phenotype in cells transfected with VP1ΔBC1-2/ΔVP2 was compared with the diffuse staining in the corresponding VP1ΔBC1-2/VP2 mutant, an effect also observed in other VP1 mutants containing the NLM domain (not shown). Therefore, the genetic removal of the BC domains triggers VP1 toward a Ub-proteasome degradation pathway. The degradation can presumably be prevented by VP2 coexpression, although a contribution to this phenomenon by the NS2 isoforms that are mutated at their carboxy-terminal domains in the ΔVP2 mutants (Fig. 1B) cannot be ruled out.

VP1 sequences are required to initiate MVMi infection. VP1 was necessary for the infection of the incoming MVM virions at an unidentified step following cell surface binding and internalization but before DNA replication (62), and the sequence homologous to BC1 in the VP1 protein of the parvovirus CPV was important for viral multiplication in culture (66). To assess the roles of the BC sequences of VP1 in the initiation of MVM infection, the specific infectivity of MVMi virions with mutations or deletions in the BC sequences was compared to that of the parental MVMi virus. VP1 mutant genomes, harboring the wt VP2 sequence to ensure efficient nuclear transport and caspid assembly of synthesized proteins (Fig. 4), were transfected on a large scale into permissive NB324K cells, and intracellular particles were harvested 48 h afterwards (see Materials and Methods). All BC mutant genomes replicated and yielded empty and DNA-filled particles that could be purified by equilibrium centrifugation through density gradients (not shown). Therefore, none of the BC sequences were essential for the late steps of the viral life cycle, including genome encapsidation. To test the specific infectivity of the purified DNA-filled virions, their capacities to initiate infection were quantitatively determined by measuring viral DNA and VP protein synthesis in cells inoculated with a normalized number of particles (Fig. 6). Mutant virions efficiently associated with NB324K cells at the end of the adsorption period (0 h p.i.), as did the wt, suggesting that the BC sequences are not involved in binding to the cells. However, late in the normal infection cycle (24 h p.i.), only the wt virions yielded a large number of DNA replicative forms (RF1 and RF2), in contrast with the absent or the barely detectable DNA amplification noted in any of the VP1 mutants. As a second test of infectivity, the numbers of cells showing de novo VP synthesis (fluorescent focus) in a single round of infection with normalized inocula of purified virions were compared (Fig. 6B). A high number of cells undergoing patent VP synthesis was demonstrable in monolayers inoculated with the wt virions by 24 h p.i., but the number of fluorescent foci for any of the VP1 mutant virions ranged between 20- and 100-fold lower. The low specific infectivities of the virions carrying the ΔBC1, ΔBC1-2, and ΔBC2-4 mutations compared to that of the wt indicated that the BC1 and BC2-4 sequences have specific functions in the infectivity of MVMi that may operate prior to nuclear targeting. However, unlike their roles in the nuclear translocation of VP subunits (Fig. 3), none of the BC sequences nor the NLM domains suffice for the incoming MVMi particle to initiate the infection.

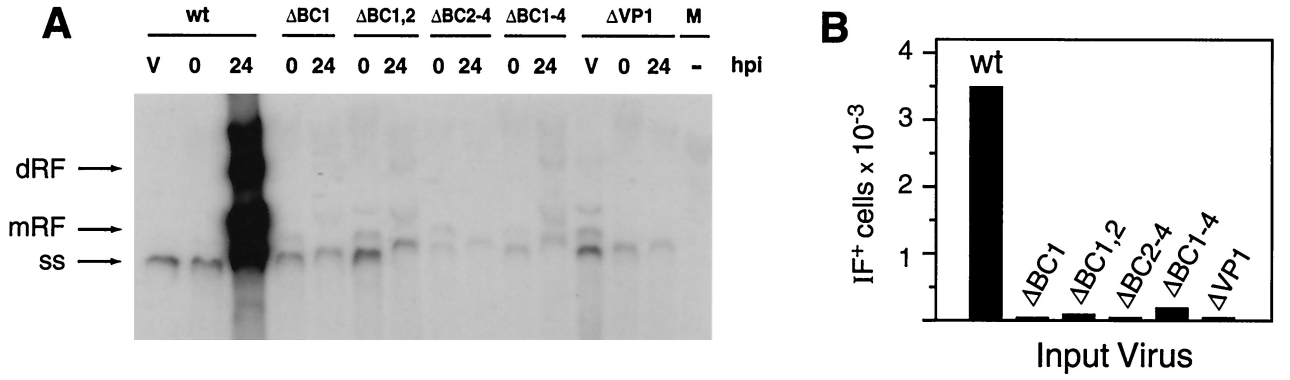

FIG. 6. Roles of the BC sequences of VP1 in the onset of infection. Plasmid constructs harboring the wt VP2 protein sequence and the indicated genetic changes in the VP1-specific sequence were transfected into NB324K cells, and intracellular DNA-filled virions were harvested and purified by CsCl gradients. (A) Viral DNA amplification. Monolayers of 10^6 NB324K cells were inoculated with the purified virions, and cell-associated low-molecular-weight DNA was isolated at 0 and 24 h p.i. (lanes 0 and 24) and analyzed by Southern blotting with a ^{32}P-labeled MVM probe. Exposure was for 48 h with intensifying screening at −70°C. Lanes V, viral genomes extracted from purified particles; lanes M, mock-infected cultures. Purified BC mutant virions contained various amounts of mRF as previously described for ΔVP1 virions (62), the meaning of which is unclear. ss, single-stranded viral genomes. (B) IF analysis of virion infectivity. Cells grown on coverslips were inoculated with normalized numbers of the indicated purified virions and 24 h afterward fixed and stained by IF with VP antiserum. The numbers of scored cells showing VP synthesis are the averages of two independent inoculations.

DISCUSSION

This work describes the nature of the sequences allowing nuclear access to the capsid proteins of the parvovirus MVMi at two stages of the virus life cycle, as newly synthesized proteins in the infection and in the incoming infectious particle. The data indicate that some of the identified NLS function in both processes while others are specific for either of the transport events. Therefore, the routes of transport of the VP supramolecular entities reaching the nucleus during MVMi infection must at least partly differ.

Nuclear transport and assembly of MVM capsid proteins. Although the two capsid proteins of MVM share the entire amino acid sequence except for the 142 amino acids of the VP1 N-terminal region, the main *cis*-acting NLS regulating their nuclear transport differ in the two polypeptides. VP1 translocated to the nucleus mainly by the activity of the BC1 and NLM domains placed toward both ends of the polypeptide, while BC2 was necessary to a minor extent for full nuclear transport capacity (Fig. 2). Each of the BC1 and BC2 domains matches conventional NLS in the single-stretch disposition (33, 34), and indeed, it was previously shown that a CPV peptide corresponding to BC1 sufficed for nuclear transport to a heterologous protein, whereas peptides corresponding to the other BC sequences were not active in microinjection assays (64). Similarly, BC3 and BC4 did not show transport activity for VP1 in the context of the complete MVM genome (Fig. 2). VP2 lacks BC sequences, and its nuclear transport exclusively mediated by the proper configuration of the NLM was sensitive to deletions across the VP1/VP2 common sequence (38). The fact that VP1 mutants, such as VP1ΔBC1-2/ΔVP2 or VP1ΔBC1-4/ΔVP2, with high nuclear targeting capacity but unable to form capsids (Fig. 2 and 4) were absolutely retained in the cytoplasm by point mutations introduced at the NLM sequence (Fig. 2, mutants VP1ΔBC12ΔNLM/ΔVP2 and VP1ΔBC14ΔNLM/ΔVP2) further reinforces the nature of the NLM as a structured nuclear transport domain dissociable from capsid formation functions.

Despite the inherent capacities of VP1 and VP2 to independently target the nucleus, the contributions of their NLS must be understood in the context of the VP complexes that are formed in the cytoplasm for cotransport. The efficient cooperative VP1/VP2 interaction was reciprocally probed by the capacity of VP2 subunits to fully carry into the nucleus partly incompetent VP1 subunits (mutant VP1ΔBC1-4/VP2 [Fig. 3]) and by the increased nuclear transport of incompetent VP2 subunits by the BC activity of VP1 (mutant VP1ΔNLM/VP2ΔNLM). Therefore, it was very significant that the BC1 and BC2 sequences of VP1 and the NLM of VP2 also showed nuclear targeting activity in the cotransport assays (Fig. 3). Cotransfection experiments between the VP1ΔBC1-4/ΔVP2 and the ΔVP1/VP2ΔNLM plasmids aimed at assessing whether the NLM of VP1 provides transport activity for VP1/VP2 complexes gave inconsistent results due to the varied VP1/VP2 ratio of expression in the transfected population (not shown), yet its functioning for singly expressed VP1 proteins (Fig. 2) may suggest some transport capacity for VP complexes as well. Therefore, besides the VP2-only oligomer, the transport-competent VP1/VP2 oligomer should contain the BC1 and the BC2 of VP1, and the NLM of both proteins, in a functional configuration exposed to the cellular transport machinery. We have previously hypothesized that such an oligomer may be a trimer based on the extension of VP cooperative interaction at the VP1/VP2 ratio of expression (38) (Fig. 3).

The formation of the MVM capsid required nuclear localization and VP2 contribution, as neither mutant VP subunits retained in the cytoplasm nor nuclear accumulations of structural proteins without the concourse of wt VP2 subunits showed signs of capsid assembly. The requirement for the nuclear milieu in order for capsids to form was also reported for the parvovirus adeno-associated virus (30), though in heterologous insect cellular systems with inefficient VP2 nuclear

transport a small fraction of the accumulated protein can assemble into capsids at the nuclear periphery (reference 70 and our unpublished observations). The capacity of VP2 to assemble in capsids while VP1 cannot under similar high nuclear accumulation (Fig. 3) may be understood, since inspection of the available MVMi crystal structure (1) reveals that the core of the T=1 parvovirus capsid cannot accommodate 60 142-amino-acid-long fragments of the VP1-specific N-terminal sequence (M. G. Rossmann, personal communication), a physical constraint that may also restrict the assembly of the nuclear deletion mutants lacking up to 50 VP1 residues (Fig. 4, mutant VP1ΔBC1-4/ΔVP2). We have not further investigated the minimal VP size that can be tolerated in the MVM capsid or whether a particular VP1 N-terminal sequence hampers assembly. In addition, the assembly of the MVM icosahedral capsid must require proper folding of the protein subunits that VP1 may not configure by itself. This hypothesis is supported by the finding that the accumulation of Ub-VP1 in the cytoplasm and in the nucleus induced by the ΔBC1-2 and especially the ΔBC1-4 mutant proteins could be significantly prevented by the coexpression of cytoplasmic (ΔNLM) or transport-competent VP2 proteins (Fig. 5 shows cytoplasmic examples). The Ub-tagged VP1 mutants should be substrates recognized and degraded by the 28S proteasome (19) following a selective degradation pathway common to many proteins in the eukaryotic cell (29). While the mechanisms triggering ubiquitination and the sites of Ub chain elongation in VP1 remain to be investigated, the capacity of VP2 to prevent ubiquitination suggests its role as a chaperone masking domains susceptible to ubiquitination or assisting VP1 folding in the cytoplasm. Altogether, the data so far are consistent with our proposed model of NLS and NLM being formed in cytoplasmic VP oligomers to order the subsequent MVM nuclear capsid assembly (38).

Functions of VP nuclear targeting sequences in the onset of infection. The size of the parvovirus capsid (25 nm) is close to the functional exclusion limit of the NPC (22), and thus, the particle could theoretically reach the nucleus in an essentially intact configuration (68). If so, the nuclear targeting sequences assigned for the VP proteins (Fig. 2 and 3) could not be used by a coated incoming virion to interact with the transport machinery, since the NLM domain is disposed at the inner surface of the capsid (1) and the VP1 N-terminal-specific sequence is inaccesible to antibodies and to proteases in the intact particles (15, 59). However, the BC1-to-BC4 sequences of VP1 were strictly required for the virus to initiate DNA replication and gene expression (Fig. 6). Therefore, there must be a certain distortion of the configuration or a disassembly of the capsid during the intracellular traffic of the autonomous parvovirus from the cellular surface to the nucleus (49, 65) to allow the entire 142-amino-acid region of VP1 to be externalized and to assist in viral genome delivery. Interestingly, MVM and CPV virions heated and treated with urea in vitro can expose VP1-specific sequence without apparent disassembly (15, 66), a process that may be biologically relevant, as heat can also specifically mimic the conformational transition that exposes the N-terminal region of VP2 triggered by genome encapsidation (28). Furthermore, the VP1 N-terminal end was exposed in CPV virions traversing toward the nucleus, as they were neutralized with VP1-specific microinjected antibodies (66). Thus, it is conceivable that the incoming virus traverses the NPC prior to disassembly by the functions of the BC sequences exposed in an unfolded VP1 N-terminal domain. However, although VP2 was not sufficient for the infectivity of the incoming virions (62) (Fig. 6), the participation of the NLMs of VP2 and VP1 in this process is unclear, since the preparation of VP1 mutant virions (Fig. 6) required transport-competent NLM-bearing VP2 subunits. Thus, in an alternative mechanism, the NLM may cooperate with the BC sequences for viral genome delivery into the nucleus from a stable disassembly intermediate in which the β-strand configuration of this domain is maintained.

The BC sequences, highly conserved among parvoviruses (62), should be required for the several processes mediated by the VP1-specific sequence to initiate infection. The perfect homology of the BC1 and BC2 nuclear transport domains (Fig. 2 and 3) necessary for MVMi particle infectivity (Fig. 6) with consensus NLS that bind karyopherin α/β receptors (33, 34, 54) strongly suggests that parvoviruses use factors of this transport pathway to dock their genomes to the NPC in association with VP1. In addition, VP1-specific sequence contains a phospholipase A_2 (PLA_2) active domain lying between BC1 and BC2 required for the transfer of the parvovirus genome from late endosomes or lysosomes to the nucleus (71). Although our mutational analysis did not target the PLA_2 domain, the deletions created in some mutant virions showing a defect in infection (Fig. 6) may be caused by an indirect effect on the proper folding of the polypeptide to display phospholipase activity. Finally, the nature of the activities provided by the BC3 and BC4 sequences lacking recognizable nuclear targeting capacity for VP1 subunits (Fig. 2 and 3), but essential to initiate infection (Fig. 6), remains to be found. It may be worthwhile to hypothesize that some BC mutant virions fail in infection by ubiquitination of the incoming MVM particle, as mentioned above for the VP1 mutant subunits synthesized de novo (Fig. 5). Interestingly, tissue-specific ubiquitination of the entering adeno-associated virus virions after endocytosis was proposed as a mechanism controlling parvovirus tropism (20). The documented determination of the autonomous parvovirus tropism by a few amino acids of VP2 (3, 26, 50, 41) on the incoming particle surface (5, 25) that possibly act at the uncoating step (52) may be related to the capacity of VP2 to prevent VP1 ubiquitination described above (Fig. 5). If so, entering parvovirus virions would be ubiquitinated at the exposed VP1 domain in nonpermissive cells due to a disorder or premature uncoating. In summary, the nuclear targeting of the small parvovirus capsid involves multiple sequences of a structurally dynamic coat leading to complex interactions with the transport machinery and other basic regulatory processes of cell biology.

ACKNOWLEDGMENTS

E.L. and J.C.R. contributed equally to this work.

We are indebted to P. Tattersall (Yale University, New Haven, Conn.) for providing the MVMi infectious plasmid and the VP1-specific polyclonal antibody and for generous intellectual support, to C. Parrish (Cornell University, Ithaca, N.Y.) for the anti-MVM MAb, and to J. Valcárcel (European Molecular Biology Laboratory, Heidelberg, Germany) for advice on splicing mutagenesis. The technical support of C. Sánchez for confocal microscopy is also gratefully acknowledged.

This work was supported by grants SAF 98-0019 and CICYT from the Spanish Ministery of Science and 08.2/0008.1/2000 from the Community of Madrid and by an institutional grant from Fundación Ramón Areces to the Centro de Biología Molecular "Severo Ochoa." E.L. was supported by a predoctoral fellowship from the Spanish Ministry of Education.

REFERENCES

1. **Agbandje-McKenna, M., A. Llamas-Saiz, F. Wang, P. Tattersall, and M. G. Rossmann.** 1998. Functional implications of the structure of the murine parvovirus minute virus of mice. Structure **6:**1369–1381.
2. **Antón, L. C., U. Schubert, I. Bacík, M. F. Princiotta, P. A. Wearsch, J. Gibbs, P. M. Day, C. Realini, M. C. Rechsteiner, J. R. Bennink, and J. W. Yewdell.** 1999. Intracellular localization of proteasomal degradation of a viral antigen. J. Cell Biol. **146:**113–124.
3. **Antonietti, J.-P., R. Sahli, P. Beard, and B. Hirt.** 1988. Characterization of the cell type-specific determinant in the genome of minute virus of mice. J. Virol. **62:**552–557.
4. **Astell, C. R., M. E. Gardinerd, and P. Tattersall.** 1986. DNA sequence of the lymphotropic variant of minute virus of mice, MVM(i), and comparison with the DNA sequence of the fibrotropic prototype strain. J. Virol. **57:**656–669.
5. **Ball-Goodrich, L. J., and P. Tattersall.** 1992. Two amino acid substitutions within the capsid are coordinately required for acquisition of fibrotropism by the lymphotropic strain of minute virus of mice. J. Virol. **66:**3415–3423.
6. **Berns, K. I.** 1996. Parvoviridae: the viruses and their replication. *In* B. N. Fields et al. (ed.), Virology, p. 2173–2197. Lippincott-Raven, Philadelphia, Pa.
7. **Boissy, R., and C. R. Astell.** 1985. An Escherichia coli recBC sbc BrecF host permits the deletion-resistant propagation of plasmid clones containing the 5′-terminal palindrome of minute virus of mice. Gene **35:**179–185.
8. **Bonnard, G. D., E. K. Manders, D. A. Campbell, R. B. Herberman, and M. J. Collins.** 1976. Immunosuppressive activity of a subline of the mouse EL-4 lymphoma. J. Exp. Med. **143:**187–205.
9. **Bouyac-Bertoia, M., J. D. Dvorin, R. A. M. Fouchier, Y. Jenkins, B. E. Meyer, L. I. Wu, M. Emerman, and M. H. Malim.** 2001. HIV-1 infection requires a functional integrase NLS. Mol. Cell **7:**1025–1035.
10. **Brownstein, D. G., A. L. Smith, R. O. Jacoby, E. A. Johnson, G. Hansen, and P. Tattersall.** 1991. Pathogenesis of infection with a virulent allotropic variant of minute virus of mice and regulation by host genotype. Lab. Investig. **65:**357–363.
11. **Bui, M., G. R. Whittaker, and A. Helenius.** 1996. Effect of M1 protein and low pH on nuclear transport of influenza virus ribonucleoproteins. J. Virol. **70:**8391–8401.
12. **Clemens, D. L., J. B. Wolfinbarger, S. Mori, B. D. Berry, S. F. Hayes, and M. E. Bloom.** 1992. Expression of Aleutian mink disease parvovirus capsid proteins by a recombinant vaccinia virus: self-assembly of capsid proteins into particles. J. Virol. **66:**3077–3085.
13. **Clemens, K. E., D. R. Cerutis, L. R. Bueger, C. Q. Yang, and D. J. Pintel.** 1990. Cloning of minute virus of mice cDNA and preliminary analysis of individual proteins expressed in murine cells. J. Virol. **64:**3967–3973.
14. **Cotmore, S. F., A. D'Abramo, L. Carbonell, J. Bratton, and P. Tattersall.** 1997. The NS2 polypeptide of parvovirus MVM is required for capsid assembly in murine cells. Virology **231:**267–280.
15. **Cotmore, S. F., A. M. D'Abramo, M. T. Christine, and P. Tattersall.** 1999. Controlled conformational transitions in the MVM virions expose the VP-1 N-terminus and viral genome without particle disassembly. Virology **254:** 169–181.
16. **Cotmore, S. F., and P. Tattersall.** 1987. The autonomously replicating parvoviruses of vertebrates. Adv. Virus Res. **33**:91–173.
17. **Cotmore, S. F., and P. Tattersall.** 1990. Alternate splicing in a parvoviral nonstructural gene links a common amino-terminal sequence to downstream domains which confer radically different localization and turnover characteristics. Virology **177:**477–487.
18. **Daigle, N., J. Beaudouin, L. Hartnell, G. Imrech, E. Hallberg, J. Lippincott-Schwartz, and J. Ellenberg.** 2001. Nuclear pore complexes form immobile networks and have a very low turnover in live mammalian cells. J. Cell Biol. **154:**71–84.
19. **DeMartino, G. N., and C. A Slaughter.** 1999. The proteasome, a novel protease regulated by multiple mechanisms. J. Biol. Chem. **274:**22123–22126.
20. **Duan, D., Y. Yue, Z. Yan, and J. F. Engelhardt.** 2000. Endosomal processing limits gene transfer to polarized airway epithelia by adeno-associated virus. J. Clin. Investig. **105:**1573–1587.
21. **Everett, R. D.** 2000. ICPO induces the accumulation of conjugated ubiquitin. J. Virol. **74:**9994–10005.
22. **Feldherr, C. M., E. Kallenbach, and N. Schultz.** 1984. Movement of a karyophilic protein through the nuclear pore of oocytes. J. Cell Biol. **99:** 2216–2222.
23. **Fujimuro, M., H. Sawada, and H. Yokosawa.** 1994. Production and characterization of monoclonal antibodies specific to multi-ubiquitin chains of polyubiquitinated proteins. FEBS Lett. **349:**173–180.
24. **García-Bustos, J., J. Heitman, and M. N. Hall.** 1991. Nuclear protein localization. Biochim. Biophys. Acta **1071:**83–101.
25. **Gardiner, E. M., and P. Tattersall.** 1988. Evidence that developmentally regulated control of gene expression by a parvoviral allotropic determinant is particle mediated. J. Virol. **62:**1713–1722.
26. **Gardiner, E. M., and P. Tattersall.** 1988. Mapping of the fibrotropic and lymphotropic host range determinants of the parvovirus minute virus of mice. J. Virol. **62:**2605–2613.
27. **Green, M. R.** 1986. Pre-mRNA splicing. Annu. Rev. Genet. **20:**671–708.
28. **Hernando, E., A. L. Llamas-Saiz, C. Foces-Foces, R. Mckenna, I. Portman, M. Agbandje-McKenna, and J. M. Almendral.** 2000. Biochemical and physical characterization of Parvovirus Minute Virus of Mice virus-like particles. Virology **267:**299–309.
29. **Hershko, A., and A. Ciechanover.** 1998. The ubiquitin system. Annu. Rev. Biochem. **67:**425–479.
30. **Hoque, M., K.-I. Ishizu, A. Matsumoto, S.-I. Han, F. Arisaka, M. Takayama, K. Suzuki, K. Kato, T. Kanda, H. Watanabe, and H. Handa.** 1999. Nuclear transport of the major capsid protein is essential for adeno-associated virus capsid formation. J. Virol. **73:**7912–7915.
31. **Ishii, N., N. Minami, E. Y. Chen, A. L. Medina, M. M. Chico, and H. Kasamatsu.**1996. Analysis of a nuclear localization signal of simian virus 40 major capsid protein Vp1. J. Virol. **70:**1317–1322.
32. **Jongeneel, C. V., R. Sahli, G. K. McMaster, and B. Hirt.** 1986. A precise map of splice junctions in the mRNAs of minute virus of mice, an autonomous parvovirus. J. Virol. **59:**564–573.
33. **Kalderon, D., B. L. Roberts, W. D. Richardson, and A. E. Smith.** 1984. A short amino acid sequence able to specify nuclear location. Cell **39:**499–509.
34. **Kalderon, D., W. D. Richardson, A. F. Markham, and A. E. Smith.** 1984. Sequence requirements for nuclear location of simian virus 40 large-T antigen. Nature **311:**33–38.
35. **Kasmatsu, H., and A. Nakanishi.** 1998. How do animal DNA viruses get to the nucleus? Annu. Rev. Microbiol. **52:**627–686.
36. **Kunkel, A. K.** 1985. Rapid and efficient site-specific mutagenesis without phenotypic selection. Proc. Natl. Acad. Sci. USA **82:**488–492.
37. **Liddington, R. C., Y. Yan, J. Moulai, R. Sahli, T. L. Benjamin, and S. C. Harrison.** 1991. Structure of simian virus 40 at a 3.8-Å resolution. Nature **354:**278–284.
38. **Lombardo, E., J. C. Ramírez, M. Agbandje-McKenna, and J. M. Almendral.** 2000. A β-stranded motif drives capsid protein oligomers of the parvovirus minute virus of mice into the nucleus for viral assembly. J. Virol. **74:**3804–3814.
39. **Maroto, B., J. C. Ramírez, and J. M. Almendral.** 2000. Phosphorylation status of the parvovirus minute virus of mice particle: mapping and biological relevance of the major phosphorylation sites. J. Virol. **74:**10892–10902.
40. **Mattaj, I. W., and L. Englmeier.** 1998. Nucleocytoplasmic transport: the soluble phase. Annu. Rev. Biochem. **67:**265–306.
41. **Maxwell, I. H., A. L. Spitzer, F. Maxwell, and D. J. Pintel.** 1995. The capsid determinant of fibrotropism for the MVMp strain of minute virus of mice functions via VP2 and not VP1. J. Virol. **69:**5829–5832.
42. **McMaster, G. K., P. Beard, H. D. Engers, and B. Hirt.** 1981. Characterization of an immunosuppressive parvovirus related to the minute virus of mice. J. Virol. **38:**317–326.
43. **Michael, W. M., P. S. Eder, and G. Dreyfuss.** 1997. The nuclear shuttling domain: a novel signal for nuclear import and nuclear export in the hnRNP K protein. EMBO J. **16:**3587–3598.
44. **Morgan, W. R., and D. C. Ward.** 1986. Three splicing patterns are used to excise the small intron common to all minute virus of mice RNAs. J. Virol. **60:**1170–1174.
45. **Nakanishi, A., J. Clever, M. Yamada, P. P. Li, and H. Kasamatsu.** 1996. Association with capsid proteins promotes nuclear targeting of simian virus 40 DNA. Proc. Natl. Acad. Sci. USA **93:**96–100.
46. **Nigg, E. A.** 1997. Nucleocytoplasmic transport: signals, mechanisms and regulation. Nature **386:**779–787.
47. **Ojala, P. M., B. Sodeik, M. Ebersold, U. Kutay, and A. Helenius.** 2000. Herpes simplex virus type 1 entry into host cells: reconstitution of capsid binding and uncoating at the nuclear pore complex in vitro. Mol. Cell. Biol. **20:**4922–4931.
48. **Paradiso, P. R., K. R. Williams, and R. L. Constantino.** 1984. Mapping of the amino terminus of the H-1 parvovirus major capsid protein. J. Virol. **52:**77–81.
49. **Parker, J. S., and C. R. Parrish.** 2000. Cellular uptake and infection by canine parvovirus involves rapid dynamin-regulated clhatrin-mediated endocytosis, followed by slower intracellular trafficking. J. Virol. **74:**1919–1930.
50. **Parrish, C. R., and L. E. Carmichael.** 1986. Characterization and recombination mapping of an antigenic and host range mutation of canine parvovirus. Virology **148:**121–132.
51. **Pollard, V. W., W. M. Michael, S. Nakielny, M. C. Siomi, F. Wang, and G. Dreyfuss.** 1996. A novel receptor-mediated nuclear protein import pathway. Cell **86:**985–994.
52. **Previsani, N., S. Fontana, B. Hirt, and P. Beard.** 1997. Growth of the parvovirus minute virus of mice MVMp3 in EL4 lymphocytes is restricted

after cell entry and before viral DNA amplification: cell-specific differences in virus uncoating in vitro. J. Virol. **71:**7769–7780.
53. **Ramírez, J. C., A. Fairén, and J. M. Almendral.** 1996. Parvovirus Minute Virus of Mice strain i multiplication and pathogenesis in the newborn mouse brain is restricted to proliferative areas and to migratory cerebellar young neurons. J. Virol. **70:**8109–8116.
54. **Robbins, J., S. M. Dilworth, R. A. Laskey, and C. Dingwall.** 1991. Two interdependent basic domains in nucleoplasmin nuclear targeting sequence: identification of a class of bipartite nuclear targeting sequence. Cell **64:**615–623.
55. **Schaap, P. J., J. V. Riet, C. L. Woldringh, and H. A. Raué.** 1991. Identification and functional analysis of the nuclear localization signals of ribosomal protein L25 from *Saccharomyces cerevisiae*. J. Mol. Biol. **221:**225–237.
56. **Schoborg, R. V., and D. Pintel.** 1991. Accumulation of MVM gene products is differentially regulated by transcription initiation, RNA processing and protein stability. Virology **181:**22–34.
57. **Segovia, J. C., J. M. Gallego, J. A. Bueren, and J. M. Almendral.** 1999. Severe leukopenia and dysregulated erythropoiesis in SCID mice persistently infected by the parvovirus minute virus of mice. J. Virol. **73:**1774–1784.
58. **Stoffler, D., B. Fahrenkrog, and U. Aebi.** 1999. The nuclear pore complex: from molecular architecture to functional dynamics. Curr. Opin. Cell Biol. **11:**391–401.
59. **Tattersall, P., A. J. Shatkin, and D. C. Ward.** 1977. Sequence homology between the structural polypeptides of minute virus of mice. J. Mol. Biol. **111:**375–394.
60. **Trotman, L., N. Mosberger, M. Fornerod, R. Stidwill, and U. F. Greber.** 2001. Import of adenovirus DNA involves the nuclear pore complex receptor CAN/Nup214 and histone H1. Nat. Cell Biol. **3:**1092–1100.
61. **Tsao, J., M. S. Chapman, M. Agbandje, W. Keller, K. Smith, H. Wu, M. Luo, T. J. Smith, M. G. Rossmann, R. W. Compans, and C. R. Parrish.** 1991. The three-dimensional structure of canine parvovirus and its functional implications. Science **251:**1456–1464.
62. **Tullis, G. E., R. B. Lisa, and D. J. Pintel.** 1993. The minor capsid protein VP1 of the autonomous parvovirus minute virus of mice is dispensable for encapsidation of progeny single-stranded DNA but is required for infectivity. J. Virol. **67:**131–141.
63. **Van Loo, N.-D., E. Fortunati, E. Ehlert, M. Rabelink, F. Grosveld, and B. J. Scholte.** 2001. Baculovirus infection of nondividing mammalian cells: mechanisms of entry and nuclear transport of capsids. J. Virol. **75:**961–970.
64. **Vihinen-Ranta, M., L. Kakkola, A. Kakela, P. Vilja, and M. Vuento.** 1997. Characterization of a nuclear localization signal of canine parvovirus capsid proteins. Eur. J. Biochem. **250:**389–394.
65. **Vihinen-Ranta, M., W. Yuan, and C. R. Parrish.** 2000. Cytoplasmic trafficking of the canine parvovirus capsid and its role in infection and nuclear transport. J. Virol. **74:**4853–4859.
66. **Vihinen-Ranta, M., D. Wang, W. S. Weichert, and C. R. Parrish.** 2002. The VP1 N-terminal sequence of canine parvovirus affects nuclear transport of capsids and efficient cell infection. J. Virol. **76:**1884–1891.
67. **Wang, P., P. Palese, and R. E. O'Neill.** 1997. The NPI-1/NPI-3 (karyopherin α) binding site on the influenza A virus nucleoprotein NP is a nonconventional nuclear localization signal. J. Virol. **71:**1850–1856.
68. **Whittaker, G. R., M. Kann, and A. Helenius.** 2000. Viral entry into the nucleus. Annu. Rev. Cell Dev. Biol. **16:**627–651.
69. **Wistuba, A., A. Kern, S. Weger, D. Grimm, and J. A. Kleinschmidt.** 1997. Subcellular compartmentalization of adeno-associated virus type 2 assembly. J. Virol. **71:**1341–1352.
70. **Yuan, W., and C. R. Parrish.** 2001. Canine parvovirus capsid assembly and differences in mammalian and insect cells. Virology **279:**546–557.
71. **Zadori, Z., J. Szelei, M.-C. Lacoste, Y. Li, S. Garriepy, P. Raymond, M. Allaire, I. R. Nabi, and P. Tijssen.** 2001. A viral phospholipase A_2 is required for parvovirus infectivity. Dev. Cell **1:**291–302.
72. **Zennou, V., C. Petit, D. Guetard, U. Nerhbass, L. Montagnier, and P. Charneau.** 2000. HIV-1 genome nuclear import is mediated by a central DNA flap. Cell **101:**173–185.